Journal of Young Pharmacists, 2026; 18(3):741-754.
https://www.jyoungpharm.org

Original Article

Poloxamer-Based Thermosensitive Nanoparticle *in situ* Gel for Sustained Pulmonary Anti-Tubercular Drug Delivery

Pooja Singh[1], Bhavna Kumar[1,*], Santosh Kumar Verma[2]

[1]Faculty of Pharmacy, DIT University, Dehradun, Uttarakhand, INDIA.
[2]Faculty of Pharmacy, Quantum University, Roorkee, Uttarakhand, INDIA.

ABSTRACT

Background: Tuberculosis treatment requires prolonged multidrug therapy, often associated with poor patient compliance and systemic side effects. The present study aimed to develop and optimize a Poloxamer 407-based thermosensitive nanoparticle-loaded *in situ* gel system for sustained pulmonary delivery of first-line anti-tubercular drugs. **Materials and Methods:** Drug-loaded sodium alginate nanoparticles containing isoniazid, rifampicin, moxifloxacin HCl, and pyrazinamide were prepared by emulsification and incorporated into thermosensitive *in situ* gels using varying concentrations of Poloxamer 407 (18-21% w/w). The formulations were evaluated for gelation temperature, pH, viscosity, drug entrapment efficiency, *in vitro* drug release, and *in vivo* pharmacokinetic performance. **Results:** The optimized formulations containing 20% Poloxamer 407 exhibited suitable gelation temperatures (30.79-32.89°C), acceptable pH (5.22-5.55), and viscosity (2260 ± 2.08 to 3144 ± 4.04 cps). High drug entrapment efficiencies (>98%) and sustained drug release (93-99% over 12 hr) were achieved. *In vivo* pharmacokinetic studies demonstrated prolonged systemic exposure, increased half-life, and improved bioavailability compared with conventional oral drug solutions. **Conclusion:** The developed nanoparticle-loaded thermosensitive *in situ* gel system demonstrated effective sustained pulmonary delivery and enhanced pharmacokinetic performance of anti-tubercular drugs. This platform may improve therapeutic efficacy, reduce dosing frequency, and enhance patient compliance in tuberculosis management.

Keywords: Nanoparticles, Poloxamer 407, Pulmonary Drug Delivery, Sustained Release, Thermosensitive *in situ* Gel, Tuberculosis Therapy.

Correspondence:
Dr. Bhavna Kumar
Faculty of Pharmacy, DIT University, Makka Wala, Dehradun-248009, Uttarakhand, INDIA.
Email: bhavnano@gmail.com

Received: 17-04-2026;
Revised: 09-06-2026;
Accepted: 26-08-2026.

INTRODUCTION

Pulmonary drug delivery systems provide an effective solution for the focused treatment of TB, minimizing systemic toxicity and enhancing patient compliance. Thermoresponsive *in situ* gels with Poloxamer 407 form upon reaching physiological temperature, facilitating prolonged gel retention and sustained drug release in the lungs. The integration of nanoparticles enhances bioavailability by increasing solubility and facilitating deep penetration in the lung (Cojocaru *et al*., 2024; Kumar Subramani *et al*., 2024).

In situ gelling drug delivery systems are polymers that are kept in a liquid form before administration and then change to a gel when exposed to physiological conditions within the body. This transformation from sol to gel could be generated by some environmental triggers, e.g., pH or temperature fluctuations, sol diffusion, exposure to ultraviolet, or the presence of certain ions and biomolecules (Vigani *et al*., 2020). The great advantage of these systems is that they can gel post-injection, allowing one to reduce the dosing frequency and thus improve patient compliance and comfort. These formulations can also be combined with sophisticated carriers such as nanospheres, microspheres, liposomes and nanoemulsions that are designed to gel *in situ* (Vigani *et al*., 2020). Multiple delivery routes, including buccal, nasal, ophthalmic, oral, rectal, vaginal, intraperitoneal, parenteral, transdermal, and subcutaneous, are suitable for *in situ* gelling formulations. During early drug development, these systems enhance both local and systemic availability of emerging drug candidates, making them highly useful for building animal models quickly and cost-effectively across various therapeutic areas (Kim *et al*., 2023). Anti-tubercular drugs require long and frequent dosing, resulting in poor compliance and limited therapeutic levels at the target site. A need exists for a sustained and targeted delivery system. Developing an *in situ* gel loaded with nanoparticles may overcome these issues, but optimization of polymer composition, nanoparticle incorporation and controlled release remains a challenge (Nair *et al*., 2023). Hence,

OPEN ACCESS
Manuscript TECHNOMEDIA

DOI: 10.5530/jyp.20260381

this study aims to formulate and evaluate Poloxamer-HPMC-based *in situ* gel nanoparticle formulations containing first-line anti-tubercular drugs and to analyze the effect of polymer concentration on physicochemical and release parameters.

Although Poloxamer 407-based thermosensitive *in situ* gels have been widely explored for various delivery routes, limited studies have investigated their integration with sodium alginate-based nanoparticles for the simultaneous pulmonary delivery of multiple first-line anti-tubercular drugs. The present work introduces a combinatorial strategy involving nanoparticle encapsulation within a thermoresponsive Poloxamer-HPMC matrix to achieve improved drug stability, reduced burst release, enhanced pulmonary retention, and prolonged systemic exposure. This dual-controlled delivery approach distinguishes the present formulation from conventional single-drug or polymer-only *in situ* gel systems reported previously.

MATERIALS AND METHODS

Isoniazid and rifampicin (analytical grade) were procured from SRL Pvt. Ltd., India. Pyrazinamide (≥99% purity) was obtained from TCI Chemicals, and moxifloxacin HCl (pharmaceutical grade) was kindly supplied by Zydus Cadila Ltd., Ahmedabad, India. Poloxamer 407 (pharmaceutical grade) and HPMC K4M (viscosity grade) were procured from commercial suppliers. Sodium alginate (medium viscosity, analytical grade) was obtained from Thomas Baker, India. Light liquid paraffin and Span 80 (analytical grade) were procured from Qualikems. All other chemicals and solvents used were of analytical grade and used as received without further purification.

Nanoparticle development by emulsification

The accurately measured amount of sodium alginate was dissolved in ultrapure water while being continuously stirred at 100 rpm using a magnetic stirrer to produce sodium alginate (5%w/v). Span 80 (0.5 mL) and paraffin oil (10 mL) were blended by homogenizing at 5000 rpm for 20s. In order to dissolve the 75 mg of isoniazid, 3 mL of sodium alginate solution (5%w/v) was properly measured and vortexed for 1 min. The paraffin oil/Span 80 mixture will now contain the drug polymeric solution, which Was homogenized once more at 5000 rpm for 30s. By mixing in 1.5 mL of a 500 mM calcium chloride solution, the nano-sized range of particles was cross-linked, and the process was continued for 20 sec. Pure isopropyl alcohol (3 mL) was then added to harden the isoniazid-loaded sodium alginate nano-sized particles. They were then collected by centrifugation at 10000rpm for 30 min, and washed twice with isopropyl alcohol and once with ultrapure water (Kattar *et al.*, 2024; Sun *et al.*, 2025).

Preparation of Anti-Tubercular Drugs-loaded nanoparticle containing *In-Situ* gel

The freeze-dried nanoparticles were manually combined with the carrier in a weight ratio using a geometrical dilution technique. The formulations listed in Table 1 were prepared by physically blending the components using geometric mixing, and following each component was processed through a sieve #60. The formulations showed that suitable flow characteristics were further assessed. The prepared formulation was labelled and stored till further use. Four nanoparticle gel formulations (G1-G4) were prepared for each drug by varying the concentration of Poloxamer 407 from 18-21% w/w, while maintaining constant levels of HPMC K4M (0.1%), water (10 g) and benzalkonium chloride (0.02%) as a preservative (Table 2) (Gebreel *et al.*, 2021; Hui-Hui *et al.*, 2011). The concentration of sodium alginate (5% w/v) was selected based on preliminary optimization and literature evidence indicating that this concentration provides sufficient viscosity for stable emulsion formation, effective ionic crosslinking with calcium chloride, and improved nanoparticle integrity without excessive aggregation. Lower concentrations resulted in poor structural stability, whereas higher concentrations significantly increased viscosity and hindered efficient homogenization.

The *In-Situ* gel formulation was developed as a comparative pulmonary delivery system to evaluate the performance of nanoparticle-based powder delivery relative to the thermosensitive *in situ* gel system. This comparison enabled assessment of sustained release efficiency, pharmacokinetic behavior, and pulmonary retention between two advanced pulmonary delivery approaches.

Characterization of Developed Nanoparticles

FT-IR spectroscopy

Fourier-transform infrared measurements were made using FTIR spectroscopy. In order to collect FT-IR studies for solid or liquid compounds, respectively, an FTIR Spectrometer was used. The data were then analyzed using a transmittance technique with a resolution of 4000 - 400 cm^{-1}. FTIR spectra of isoniazid, rifampicin, moxifloxacin HCl and pyrazinamide loaded nanoparticles were recorded (Al-Amin *et al.*, 2025; Pasieczna-Patkowska *et al.*, 2025).

DSC analysis

DSC analysis of the drug and freeze-dried ATDs loaded sodium alginate nanoparticles was conducted to investigate the thermal behaviours of the drug in bulk form as well as in the nanoparticle formulation. Thermograms of the isoniazid, rifampicin, pyrazinamide, moxifloxacin HCl and freeze-dried ATDs loaded sodium alginate nanoparticles were obtained using a DSC SETARAM (Model: SETLINE DSC). Each sample was weighed and transferred to the aluminium pan, followed by crimping employing the crimper and heated from 30°C to 400°C at a heating rate of 10°C min^{-1}. The DSC thermogram was

captured and investigated (El-Houssiny *et al.*, 2016; Gill *et al.*, 2010; Presbítero-Espinosa *et al.*, 2021).

X-ray Diffraction

X-ray Diffraction (XRD) of the drug and freeze-dried ATDs loaded sodium alginate nanoparticles was accessed to investigate the crystalline and amorphous nature of drug and test formulation employing an PXRD Empyrean (Malvern). The XRD patterns were collected over an angular range 2θ (5°-60°) (Ali *et al.*, 2023; Ingham, 2015; Patel *et al.*, 2024).

Determination of Gelation Temperature

The gelation temperature of the formulated *in situ* gels was ascertained utilizing the tube inversion technique. A 10 mL clear glass tube carrying 5 mL of the formulation was positioned in a thermostatically regulated water bath. The temperature was incrementally raised from 20°C to 60°C at a rate of 1°C per minute, accompanied by constant mild agitation every 30 sec. The temperature at which the formulation ceased to flow upon inversion of the tube and formed a stable gel was recorded as the gelation temperature. Readings were taken in triplicate, and the mean ± standard deviation was calculated (Nasra *et al.*, 2017; Tripathi *et al.*, 2025).

Measurement of pH

The pH of the prepared *in situ* gel was assessed using a digital pH meter, calibrated with standard buffer solutions at pH 4.0, 7.0, and 9.2. Approximately 10 mL of the formulation was deposited into a beaker and allowed to equilibrate for 2 min at ambient temperature. The electrode was submerged in the sample, and the pH was documented upon achieving a stable reading. Measurements were performed in triplicate, and mean ± SD results were computed (Garala *et al.*, 2013).

Determination of Viscosity

A Brookfield viscometer with wheel No. 64 turned at 100 rpm was used to measure the viscosity of the *in situ* gel samples. The sample (20 mL) was put into the instrument's chamber and warmed up to 25°C. Readings were allowed to stabilize before the final recording. The viscosity value was recorded in centipoise (cps). Each sample was tested in triplicate, and mean ± SD values were reported (A *et al.*, 2021).

Drug Entrapment Efficiency (%)

The centrifugation method was used to find the Drug Entrapment Efficiency (DEE) of *in situ* gels loaded with nanoparticles. Centrifuge tubes were filled with a known amount of gel formulation (according to the drug content) and spun at 15,000 rpm for 30 min. Spectrophotometric analysis was performed on the obtained supernatant at the wavelength corresponding to each medication (D. Kumar *et al.*, 2013). The entrapment efficiency was calculated using the formula:

$$\text{DEE (\%)} = (\text{Total drug} - \text{Unentrapped drug}) / \text{Total drug} \times 100$$

All tests were performed in triplicate, and values are reported as the Mean ± SD.

In vitro Drug Release Studies

A Franz diffusion cell that was equipped with a dialysis membrane (MWCO: 12,000-14,000 Da) was utilized in order to carry out the *in vitro* drug release procedure. Within the donor compartment, the gel that was equivalent to the needed drug quantity was present. On the other hand, the receptor compartment was filled with Phosphate-Buffered Saline (PBS) at a pH of 7.4, maintained at 37±0.5°C, and swirled at a speed of 100 revolutions per minute. *In vitro* drug release from the nanoparticle-loaded *in situ* gel formulations was evaluated for 12 hr using the Franz diffusion cell method to assess controlled release behavior under simulated physiological conditions. Additionally, an extended-release study up to 48 hr was performed separately for comparative profiling of pure drug solutions and nanoparticle formulations to evaluate long-term release kinetics and retention characteristics (Sebe *et al.*, 2022). The cumulative drug release (%) was calculated and plotted against time.

In vivo pharmacokinetic study

Study Design

Each experimental group consisted of six animals (n=6). All animal experiments were conducted in accordance with institutional ethical guidelines and were approved by the Institutional Animal Ethics Committee (IAEC), Vivek College of Technical Education, Bijnor, under approval number VCTE/IAEC/PH/24/016. The study complied with CCSEA guidelines for the care and use of laboratory animals.

The trial involved the administration of either therapeutic doses (rifampicin 15.43 mg/kg, isoniazid 7.71 mg/kg, pyrazinamide 41.31 mg/kg, and moxifloxacin 41.31 mg/kg) or half-therapeutic doses. The quantities of each drug required for preparing the nanoparticle-loaded *in situ* pulmonary gel were calculated based on these dose variations. A rat model was used to evaluate and compare the pharmacokinetic profiles of (i) pure drug combinations administered orally, (ii) nanoparticle-loaded drug combinations formulated as an *in situ* pulmonary gel. Oral formulations were administered via intragastric gavage, pulmonary delivery was performed using a dry powder insufflator, and the pulmonary gel was administered into one nostril using a polyethylene tube attached to a microliter syringe. Blood samples were collected at 1, 2, 4, 8, 12, and 24 hr post-administration via the retro-orbital plexus. Plasma was separated by centrifugation at 1000 rpm for 20 min and filtered through a 0.45 µm membrane for analysis (Jeswani *et al.*, 2021).

Preparation of samples for HPLC analysis

The animals were bled at several time points, and the plasma obtained from each mouse was divided into two parts. The first part (100 µL) was deproteinised with 100 µL of acetonitrile, vortexed for 5 min and centrifuged at 5000×g for 20 min at 4-8ºC. The supernatant was used for analysis of RIF and moxifloxacin. The second portion of plasma (50 µL) was deproteinised with 50 µL of 10% (v/v) trichloroacetic acid, processed as above and analysed simultaneously for INH and PZA. The drugs were analysed by HPLC and compared with calibration graphs (obtained by analysing pooled blank rat plasma spiked with known drug amounts) to obtain the plasma drug concentration-time profile (Ahmad *et al*., 2005, 2006; Gerber *et al*., 2020).

Determination of drug content in lung tissue

Concurrently, animals were euthanized by cervical dislocation, and specific organs were excised, weighed individually, diced, and homogenized using a tissue homogenizer in phosphate buffer. The homogenized tissue was partitioned into two halves. The initial portion (100 µL) was subjected to deproteinization using 100 µL of acetonitrile, vortexed for 5 min, then centrifuged at 5000×g for 20 min at a temperature of 4-8ºC. The supernatant was utilized for the examination of rifampicin and moxifloxacin. The second aliquot of plasma (50 µL) was deproteinized using 50 µL of 10% (v/v) trichloroacetic acid, processed as previously described, and analyzed concurrently for INH and PZA. The pharmaceuticals were analyzed using HPLC (Petrashen *et al*., 2023; Zakaria *et al*., 2017).

Pharmacokinetic data analysis

Following administration of the Pure drug solution combination isoniazid, rifampicin, pyrazinamide and moxifloxacin through the oral route, a Nanoparticle containing combination of isoniazid, rifampicin, pyrazinamide and moxifloxacin, comprising *in situ* pulmonary gel, using the pKa solver based on the measured drug plasma concentration values. Following oral delivery, MRT, elimination rate constant, C_{max}, and T_{max} were calculated (Bekker *et al*., 2016; Ramachandran *et al*., 2023). The area under the plasma concentration-time curve from zero to the final concentration point (AUC_{0-t}) and from zero to infinity ($AUC_{0-\infty}$) were computed.

RESULTS

Characterization of developed nanoparticles

FTIR of Prepared Formulation

FTIR spectra of the physical mixtures of isoniazid, rifampicin, and moxifloxacin HCl with sodium alginate, calcium chloride, light liquid paraffin, and Span 80 were recorded in the range of 4000-400 cm^{-1} to evaluate drug-excipient compatibility Figure 1. The spectra of isoniazid showed characteristic O-H/N-H stretching (3300-3500 cm^{-1}), amide C=O stretching (1650-1670 cm^{-1}), and C-N vibrations without any significant shifts. Rifampicin exhibited typical O-H stretching (3200-3500 cm^{-1}), C=O stretching (1720-1740 cm^{-1}), and conjugated C=C vibrations, which remained unchanged in the physical mixture. Moxifloxacin HCl showed characteristic O-H/N-H stretching

Table 1: Composition of Anti-Tubercular Drugs loaded nanoparticle containing *in-situ* gel

Formulation code	Nanoparticles	Poloxamer 407 (%w/w)	HPMC K4M (%w/w)	Water (g)	Benzalkonium chloride
F1	Eqvt to 75 mg of isoniazid	18	0.1	10	0.02
F2		19	0.1	10	0.02
F3		20	0.1	10	0.02
F4		21	0.1	10	0.02
F5	Eqvt to 150 mg of rifampicin	18	0.1	10	0.02
F6		19	0.1	10	0.02
F7		20	0.1	10	0.02
F8		21	0.1	10	0.02
F9	Eqvt to 400 mg of moxifloxacin	18	0.1	10	0.02
F10		19	0.1	10	0.02
F11		20	0.1	10	0.02
F12		21	0.1	10	0.02
F13	Eqvt to 400 mg of pyrazinamide	18	0.1	10	0.02
F14		19	0.1	10	0.02
F15		20	0.1	10	0.02
F16		21	0.1	10	0.02

Table 2: Details of the animal.

Sl. No.	Group no.	Formulation name	Dose	No. of animals
1.	Group 1	Control	-	0-6
2.	Group 2	Pure drug solution combination isoniazid, rifampicin, pyrazinamide and moxifloxacin through the oral route (Through cannula)	rifampicin 15.43 mg/kg + isoniazid 7.71 mg/kg + pyrazinamide 41.31 mg/kg+ moxifloxacin 41.31mg/kg	6-12
3.	Group 3	Nanoparticle containing a combination of isoniazid, rifampicin, pyrazinamide and moxifloxacin, comprising an in situ nasal gel	Equivalent to rifampicin 15.43 mg/kg + isoniazid 7.71mg/kg + pyrazinamide 41.31 mg/kg+ moxifloxacin 41.31mg/kg	12-18

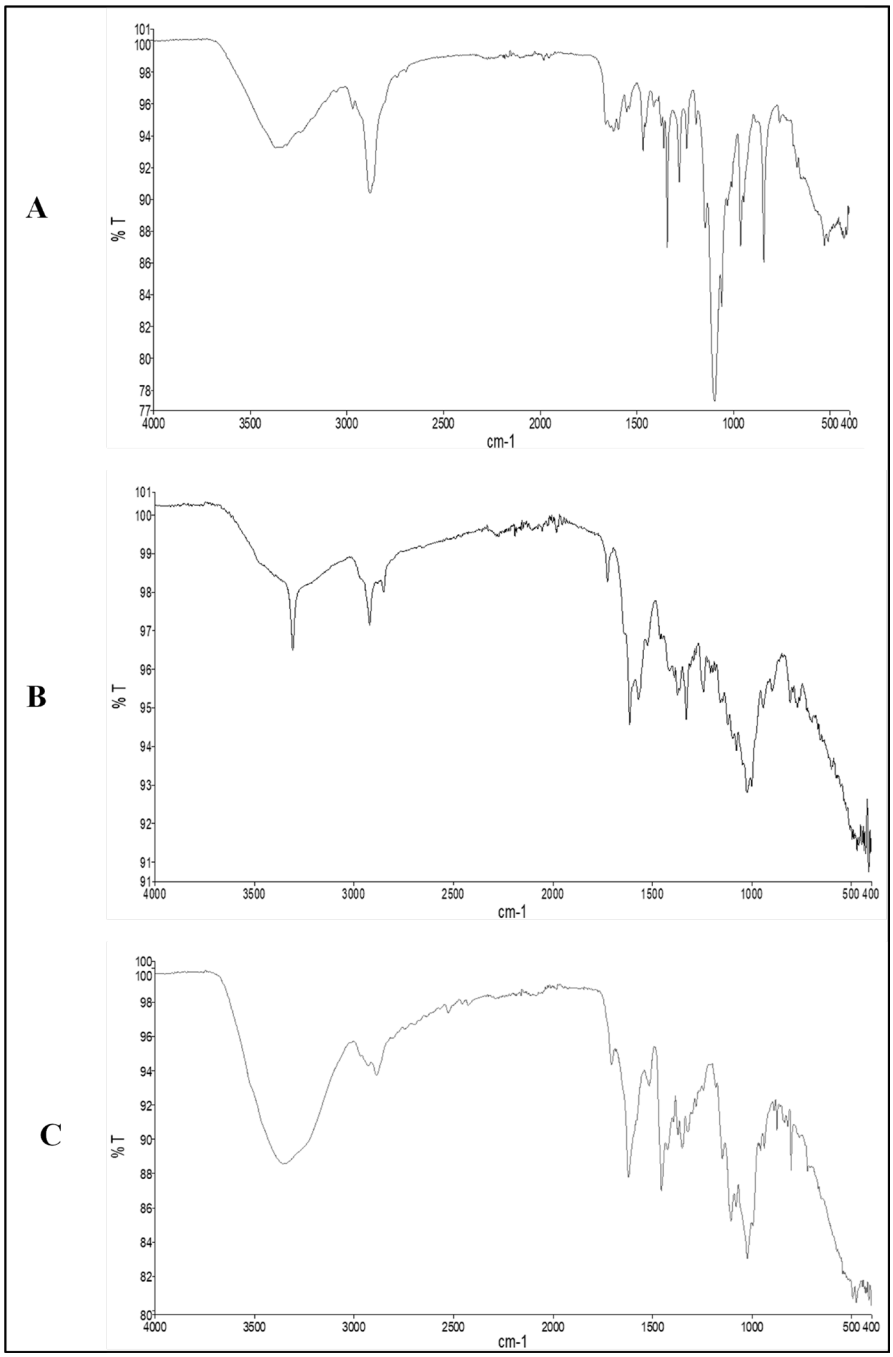

Figure 1: FTIR spectra (4000-400 cm^{-1}) of physical mixtures used for nanoparticle preparation to evaluate drug-excipient compatibility: (A) Isoniazid + sodium alginate + calcium chloride + light liquid paraffin + Span 80; (B) Rifampicin + sodium alginate + calcium chloride + light liquid paraffin + Span 80; (C) Moxifloxacin HCl + sodium alginate + calcium chloride + light liquid paraffin + Span 80.

(~3400 cm^{-1}), C=O stretching (1700-1725 cm^{-1}), and C=C/C-N vibrations (1600-1620 cm^{-1}). Sodium alginate peaks were observed in the 1000-1150 cm^{-1} region in all spectra. The absence of peak shifting, disappearance, or new peak formation confirms the chemical compatibility of all drugs with the formulation excipients.

DSC of prepared nanoparticles

Figure 2 shows the DSC thermograms of isoniazid (A), pyrazinamide (B), rifampicin (C), and moxifloxacin (D) nanoparticles, highlighting their thermal and solid-state properties. Isoniazid nanoparticles exhibited a sharp endothermic peak at 110-115°C corresponding to drug melting, with reduced enthalpy indicating partial loss of crystallinity. Pyrazinamide nanoparticles showed a melting peak at 110-120°C with slight broadening and reduced intensity, suggesting molecular dispersion and partial amorphization. Rifampicin nanoparticles displayed a broad, less intense endothermic transition around 150-165°C, reflecting significant crystallinity reduction and altered thermal behavior typical of nano-sized systems. Moxifloxacin nanoparticles showed a melting peak at 120-130°C with noticeable broadening and decreased enthalpy, indicating reduced crystalline order. The shift in melting temperatures, peak broadening, and lower enthalpy values confirm successful nanoparticle formation, decreased crystallinity, and improved drug dispersion, which are favorable for enhanced dissolution and bioavailability.

XRD

Figure 3 presents the XRD patterns of isoniazid (A), rifampicin (B), pyrazinamide (C), and moxifloxacin (D) nanoparticles. All formulations showed reduced peak intensity and significant peak broadening compared to their crystalline counterparts, indicating a loss of long-range crystalline order after nanoparticle formation. Isoniazid and rifampicin nanoparticles exhibited diffuse patterns and halo formations, suggesting a largely amorphous structure. Pyrazinamide nanoparticles showed broadened, low-intensity peaks on an amorphous background, indicating partial crystallinity. Moxifloxacin nanoparticles displayed reduced and broadened peaks, reflecting smaller crystallite size and decreased crystallinity. These results confirm the successful conversion of the drugs into amorphous or nanocrystalline forms, which is advantageous for enhancing dissolution rate and bioavailability.

Effect of Poloxamer Concentration on Gelation Temperature

Poloxamer 407 concentration plays a crucial role in controlling the gelation temperature of *in situ* gel formulations. Increasing Poloxamer concentration from 18-21% w/w significantly reduced the gelation temperature of all drug models, enabling rapid sol-to-gel transition at physiological pulmonary temperature (~37°C), ensuring efficient gel formation following pulmonary administration. This effect is attributed to the thermoreversible gelling behavior of Poloxamer, resulting from enhanced micellar aggregation and a lower critical micelle concentration at higher polymer levels. In isoniazid formulations, the gelation temperature decreased from 34.88°C (G1) to 30.74°C (G4),

Table 3: Results for Gelation Temperature, pH Viscosity, Drug Entrapment, and *in vitro* drug release.

Formulation code	Gelation temperature	pH	Viscosity (cps)	Drug entrapment (%)	*In vitro* Drug Release Studies (%)
F1	34.883±0.736	5.070±0.046	1752±4.583	90.996±0.866	92.023±0.143
F2	32.423±0.406	5.117±0.015	2091±3.786	93.882±0.901	92.848±0.432
F3	30.790±0.101	5.343±0.038	2260±2.082	99.509±0.661	99.273±0.245
F4	28.017±0.321	5.537±0.051	2515±3.055	93.593±0.433	91.724±0.851
F5	37.383±0.350	5.340±0.119	1956±2.646	92.796±0.398	90.951±0.389
F6	34.847±0.686	5.477±0.123	2251±3.215	94.056±0.699	91.0346±0.651
F7	32.893±0.300	5.553±0.095	2644±4.583	98.103±0.608	98.484±0.296
F8	28.880±0.961	5.647±0.015	2873±4.509	93.526±0.753	92.041±0.540
F9	36.607±0.906	5.050±0.087	2450±2.517	92.386±0.856	90.086±0.273
F10	33.453±0.776	5.150±0.010	2778±3.055	98.737±0.647	98.118±0.539
F11	31.783±0.818	5.220±0.020	3144±4.041	95.562±0.881	93.839±0.670
F12	28.103±0.525	5.293±0.021	3403±4.583	94.574±0.441	92.043±0.745
F13	37.930±0.791	5.149±0.056	2351±3.215	93.263±0.880	91.721±0.368
F14	33.133±0.850	5.257±0.035	2673±4.509	99.674±0.404	95.696±0.470
F15	31.507±0.946	5.353±0.055	2964±4.163	96.643±0.925	94.731±0.843
F16	27.597±0.502	5.317±0.040	3485.±4.933	96.993±0.699	95.098±0.390

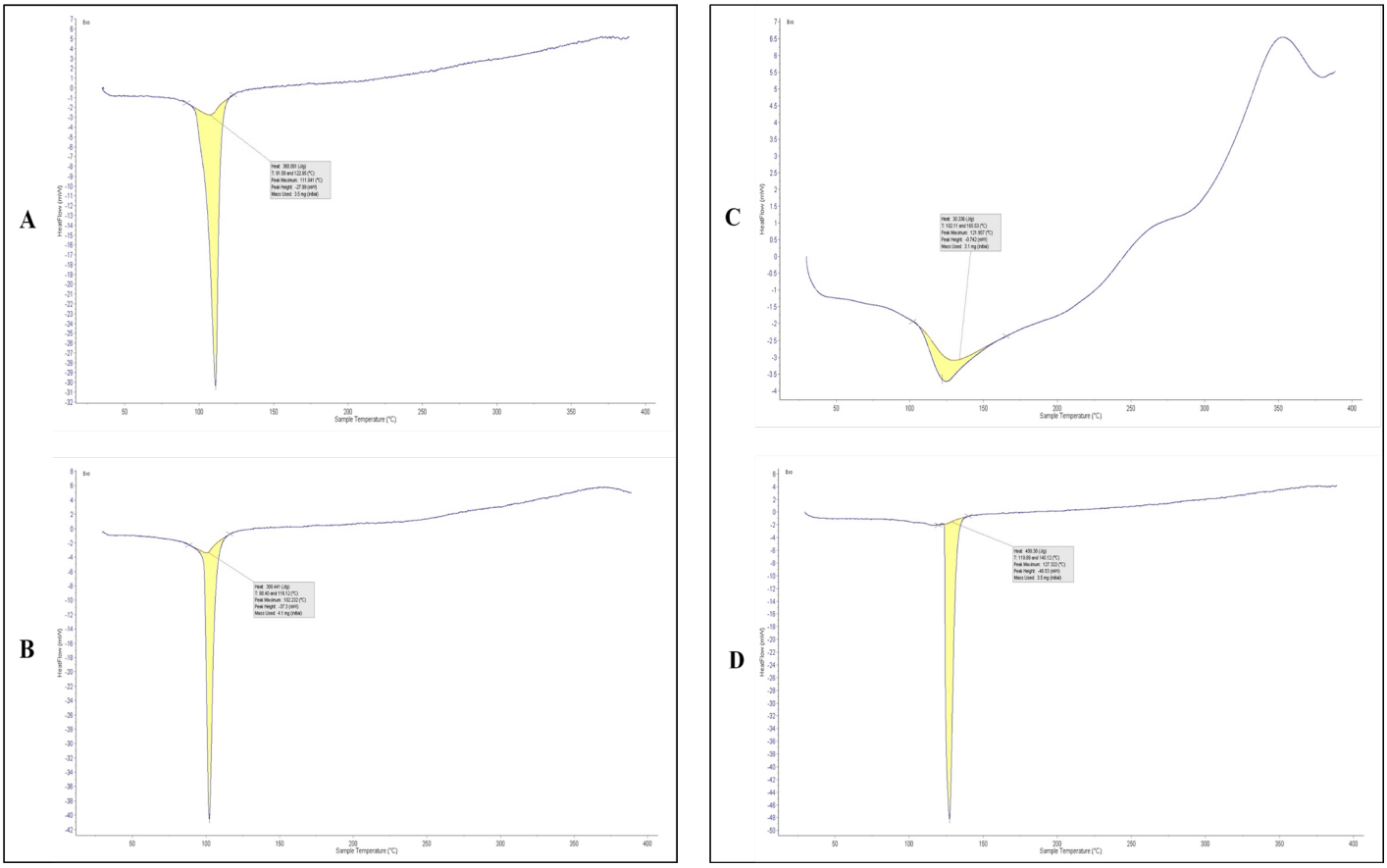

Figure 2: Differential Scanning Calorimetry (DSC) thermograms of freeze-dried sodium alginate nanoparticles loaded with anti-tubercular drugs: (A) Isoniazid nanoparticles, (B) Pyrazinamide nanoparticles, (C) Rifampicin nanoparticles, and (D) Moxifloxacin HCl nanoparticles. Samples were heated from 30-400ºC at a rate of 10ºC/min under nitrogen atmosphere.

indicating improved suitability for pulmonary delivery due to rapid gelation, enhanced mucosal adhesion, and prolonged drug retention (Table 3). Similar trends were observed with rifampicin, moxifloxacin, and pyrazinamide, confirming the consistency of this effect (Figure 4).

pH Evaluation

All formulations exhibited pH values within the acceptable physiological nasal tolerance range (5.0-6.5) making them safe for administration without causing irritation or mucosal damage. The measured pH ranged between 5.05 and 5.64, indicating that the formulations mimic natural pulmonary fluid conditions. This ensures that drug absorption occurs effectively without compromising tissue compatibility (Figure 5).

Viscosity

Viscosity is a critical parameter affecting both retention time and drug release. A direct correlation was observed between Poloxamer concentration and viscosity. As the concentration increased from 18% to 21%, the viscosity rose significantly due to increased gel strength and micellar packing density. For instance, moxifloxacin formulations demonstrated an increase from 2450 ± 2.517 cps (G1) to 3403 ± 4.583 cps (G4). Higher viscosity supports prolonged residence at the site of deposition, minimizing mucociliary clearance movement and enhancing sustained drug delivery (Figure 6).

Drug Entrapment Efficiency

All of the preparations showed high drug entrapment efficiency, with the range of 90 to 99%, which revealed the success of nanoparticles incorporation into the polymeric matrix. Optimal entrapment efficacy was realized in the G3 batches at 20% Poloxamer indicating that it was an ideal balance between the quantity of the polymer and capacity to encapsulate. In particular, highest entrapment rates of 99.509 + 0.661% with Isoniazid and 99.674 + 0.404% with Pyrazinamide were achieved showing an enhanced drug retention in the formulation system. The higher drug entrapment level at G3 level could be explained by the fact that the viscosity range was favorable and drug diffusion and leakage was minimized during the process and this way ensured the amount of drug to be incorporated in the maximum into the nanoparticles (Figure 7).

In vitro Drug Release

All formulations showed sustained drug release, confirming their suitability for controlled pulmonary drug delivery. Among them,

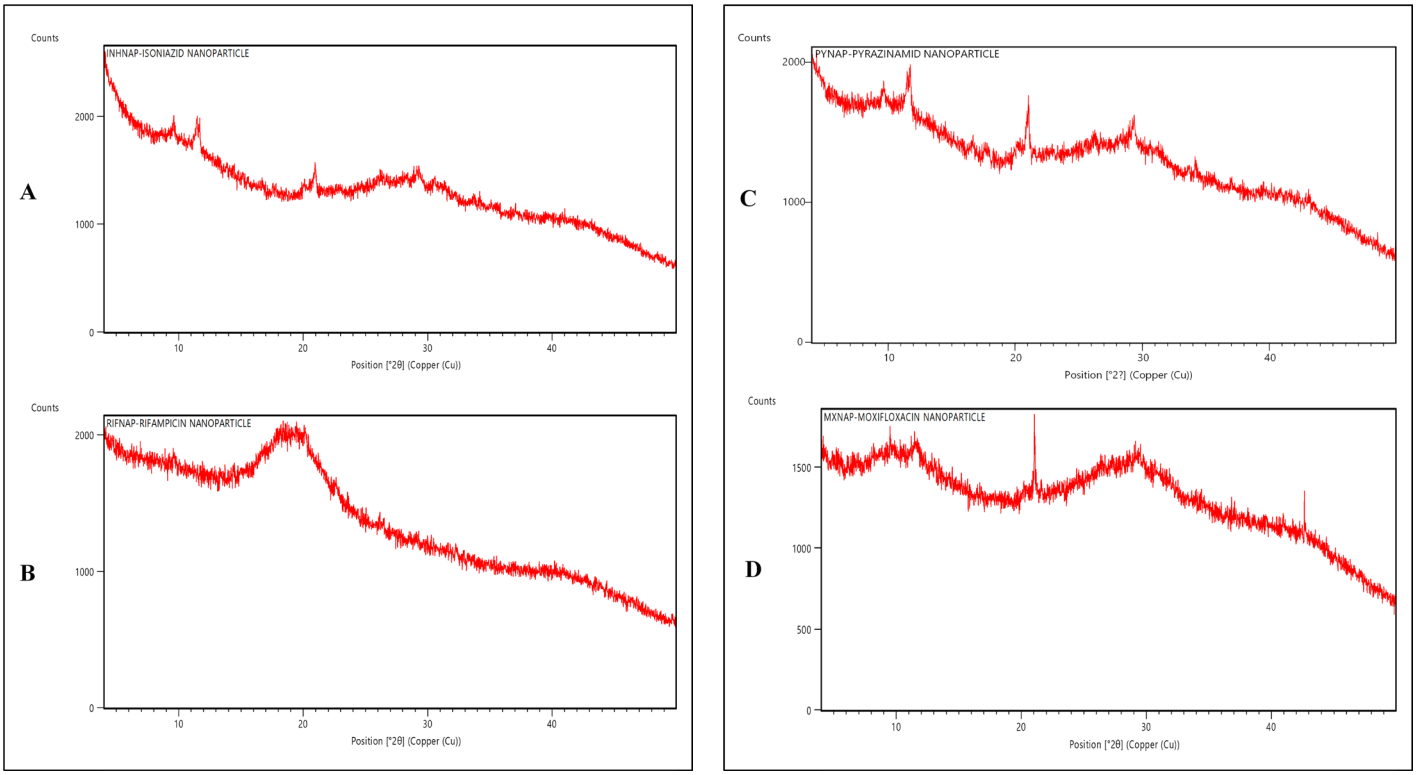

Figure 3: X-ray diffraction (XRD) patterns (2θ range: 5°-60°) of freeze-dried anti-tubercular drug-loaded sodium alginate nanoparticles: (A) Isoniazid, (B) Rifampicin, (C) Pyrazinamide, and (D) Moxifloxacin HCl nanoparticles.

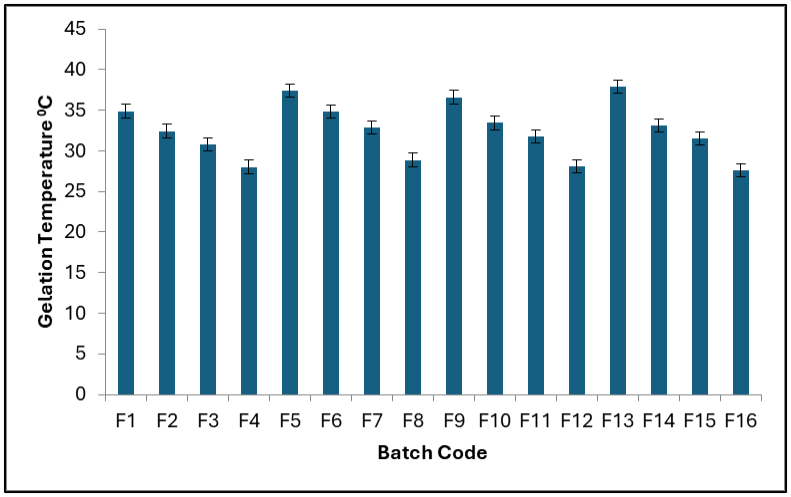

Figure 4: Effect of Poloxamer 407 concentration (18-21% w/w) on gelation temperature (ºC) of nanoparticle-loaded thermosensitive *in situ* gel formulations (G1-G4). Gelation temperature was determined using the tube inversion method (n = 3, mean ± SD). Increasing polymer concentration resulted in reduced gelation temperature, suitable for pulmonary administration (~37ºC).

the G3 formulation exhibited the highest drug release 92-99%, Figure 8 indicating an optimal balance between polymer matrix rigidity and diffusion. The intermediate viscosity of G3 allowed efficient drug diffusion without excessive restriction, unlike formulations with higher polymer concentrations (Figure 9).

Dose Response Curve

The *in vitro* drug release study showed clear differences between pure drug solutions and nanoparticle-loaded *in situ* gel formulations over 48 hr (Figure 10). Pure drug solutions exhibited a rapid initial release, indicating fast diffusion and poor retention. Isoniazid showed a low peak at 2 hr followed by a decline after 12 hr, while rifampicin, moxifloxacin HCl, and pyrazinamide showed a steady decrease. In contrast, nanoparticle-loaded *in situ* gels demonstrated a sustained and controlled release profile. All formulations showed a gradual increase in drug release up to 6-12 hr, followed by a slow decline, with significant drug levels maintained even after 48 hr. Pyrazinamide and moxifloxacin nanoparticles showed the highest cumulative release, with peaks at 12 hr and prolonged retention up to 48 hr. Overall,

nanoparticle-based *in situ* gels effectively reduced burst release and prolonged drug availability, indicating their potential advantage for sustained pulmonary or local drug delivery.

Pharmacokinetics study of optimized formulation

Pharmacokinetic analysis revealed significant differences between conventional drug solutions and nanoparticle-loaded *in situ* gel formulations. The solution forms of isoniazid and rifampicin showed short elimination half-lives (1.44 h and 5.33 hr), while moxifloxacin HCl and pyrazinamide exhibited moderately longer half-lives. In contrast, all nanoparticle *in situ* gel formulations markedly increased drug half-life, with values extending up to ~21-29 hr, indicating prolonged drug retention. The nanoparticle gels also showed delayed T_{max} and significantly higher C_{max} compared to solutions, confirming sustained and controlled drug release. Moreover, systemic exposure (AUC_{0-t} and $AUC_{0-\infty}$) was substantially enhanced, while clearance and volume of distribution were reduced. Nanoparticle-based *in situ* gels significantly improved bioavailability, prolonged circulation time, and reduced drug clearance, demonstrating superior pharmacokinetic performance over conventional solutions Table 4.

DISCUSSION

The present study successfully developed and optimized nanoparticle-loaded thermosensitive *in situ* gel systems for pulmonary delivery of first-line anti-tubercular drugs, including

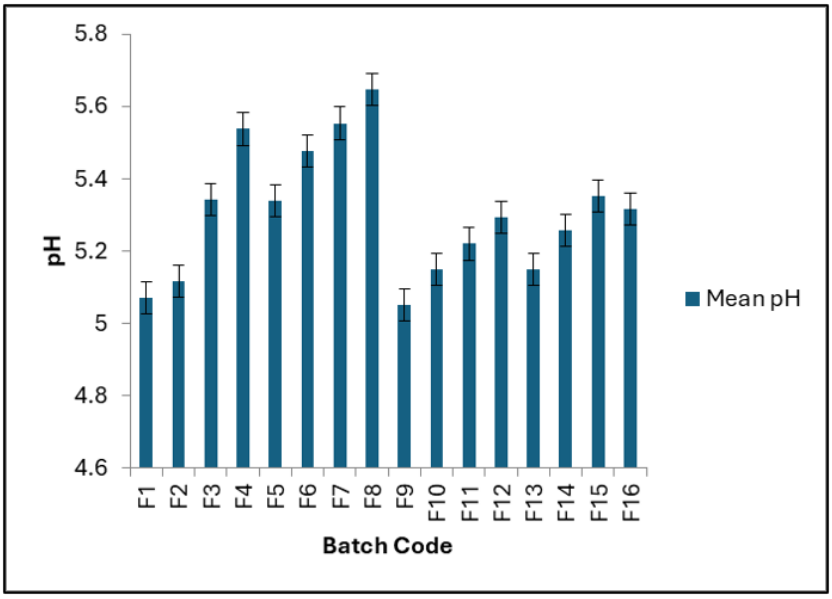

Figure 5: pH values of nanoparticle-loaded *in situ* gel formulations (G1-G4) containing varying concentrations of Poloxamer 407 (18-21% w/w). Measurements were performed at room temperature using a calibrated digital pH meter ($n = 3$, mean ± SD). All formulations showed pH within the physiologically acceptable pulmonary range.

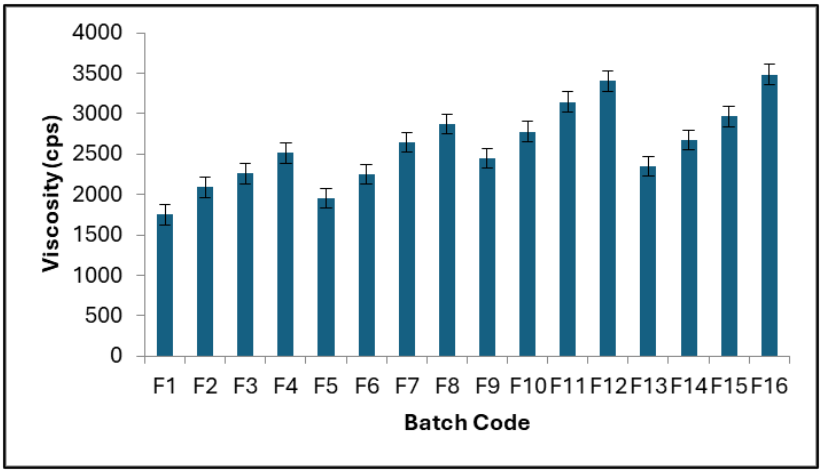

Figure 6: Viscosity (cps) of nanoparticle-loaded thermosensitive *in situ* gel formulations (G1-G4) measured using a Brookfield viscometer (Spindle No. 64, 100 rpm, 25°C; $n = 3$, mean ± SD). Viscosity increased proportionally with Poloxamer 407 concentration, contributing to improved pulmonary retention.

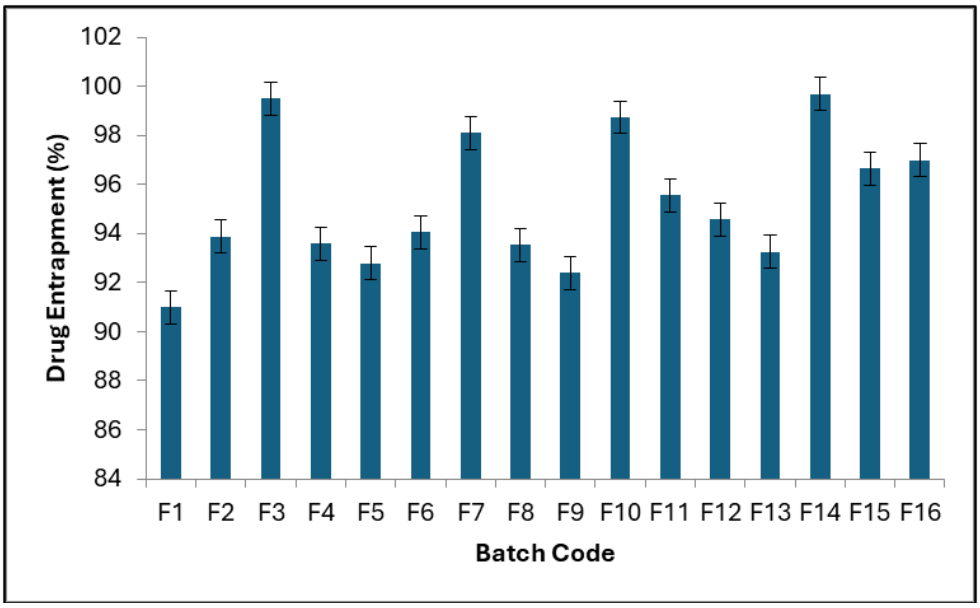

Figure 7: Drug entrapment efficiency (%) of anti-tubercular drug-loaded nanoparticle *in situ* gel formulations (G1-G4) determined by centrifugation and spectrophotometric analysis ($n = 3$, mean ± SD). Formulation G3 (20% w/w Poloxamer 407) demonstrated optimal entrapment efficiency across all drug models.

isoniazid, rifampicin, moxifloxacin HCl, and pyrazinamide. The obtained findings demonstrated that incorporation of sodium alginate nanoparticles into the Poloxamer 407-HPMC matrix significantly improved the physicochemical characteristics, sustained drug release behavior, and pharmacokinetic performance of the anti-tubercular drugs. Pulmonary drug delivery has gained considerable attention because it enables localized drug targeting, rapid absorption, reduced systemic toxicity, and improved patient compliance, particularly in chronic diseases such as tuberculosis.

The FTIR, DSC, and XRD analyses confirmed the successful incorporation of drugs into the nanoparticle matrix without significant chemical interaction between the drugs and excipients. FTIR spectra retained all characteristic functional group peaks, indicating good compatibility and formulation stability. DSC thermograms demonstrated reduced enthalpy and broadening of melting peaks, while XRD patterns exhibited reduced peak intensity and partial amorphization of the drugs after nanoparticle formation. Similar findings have been reported in nanoparticle-based pulmonary systems, where reduction in crystallinity improves drug dissolution and bioavailability due to enhanced molecular dispersion and surface area (Rosiak *et al.*, 2023; Zhang *et al.*, 2024). The conversion of crystalline drugs into partially amorphous forms may therefore contribute significantly to the enhanced release behavior observed in the present study.

Poloxamer 407 concentration played an important role in determining the thermosensitive behavior and viscosity of the formulations. Increasing polymer concentration from 18% to 21% w/w resulted in a progressive reduction in gelation temperature and an increase in viscosity. This behavior can be attributed to enhanced micellar aggregation and stronger intermolecular interactions occurring at higher polymer concentrations. The optimized G3 formulations containing 20% Poloxamer 407 showed gelation temperatures close to physiological pulmonary temperature, which is considered ideal for rapid gel formation after administration. Appropriate gelation temperature is essential to prevent premature gelation during handling while ensuring rapid transition after pulmonary delivery (Hirun *et al.*, 2022; Ullah *et al.*, 2021). The obtained pH values were within the acceptable physiological range, indicating suitability for pulmonary administration without causing irritation or mucosal damage. The formulations also demonstrated high drug entrapment efficiencies exceeding 98%, indicating effective incorporation of the anti-tubercular drugs within the nanoparticle-polymeric matrix. The optimized viscosity of G3 formulations may have minimized drug diffusion during nanoparticle preparation, thereby improving drug retention. Similar relationships between polymer viscosity and entrapment efficiency have been reported previously in nanoparticle-loaded hydrogel systems (Kumar *et al.*, 2023; Ullah *et al.*, 2021). High entrapment efficiency is important for ensuring dose uniformity, sustained drug release, and improved therapeutic performance.

In vitro release studies revealed sustained drug release profiles over 12 hr with prolonged retention up to 48 hr in extended-release studies. Compared with pure drug solutions, nanoparticle-loaded *in situ* gels effectively minimized burst release and maintained controlled drug diffusion over an extended period. The sustained release behavior can be attributed to the combined effect of sodium alginate nanoparticles and the thermosensitive gel matrix, which together create a dual-controlled diffusion barrier. This prolonged release profile is particularly beneficial in

tuberculosis therapy because conventional anti-tubercular drugs require frequent dosing and prolonged treatment durations, often resulting in poor adherence and treatment failure (Balu *et al.*, 2025; Nakmode *et al.*, 2024; Wu *et al.*, 2019). Sustained pulmonary delivery systems may therefore improve therapeutic outcomes by maintaining effective drug concentrations in the lungs for longer durations.

The *in vivo* pharmacokinetic studies further confirmed the superiority of the nanoparticle-loaded *in situ* gel formulations over conventional oral drug solutions. The optimized formulations demonstrated prolonged half-life, increased T_{max}, enhanced C_{max}, and significantly higher AUC values, indicating improved systemic exposure and prolonged circulation time. Reduced clearance and volume of distribution further supported the controlled release and retention behavior of the developed formulations. These findings are consistent with previous reports demonstrating that nanoparticle-based pulmonary delivery systems can enhance bioavailability and reduce dosing frequency through prolonged drug residence within the pulmonary region (Karemore *et al.*, 2019; Salem *et al.*, 2024). The enhanced pharmacokinetic profile observed in the present study may contribute to improved therapeutic efficacy and reduced systemic side effects during anti-tubercular therapy. The present findings demonstrate that nanoparticle-loaded thermosensitive *in situ* gels represent a promising pulmonary drug delivery platform for sustained anti-tubercular therapy. The combined advantages of nanoparticle encapsulation and thermoresponsive gelation enabled improved drug stability, controlled release, prolonged pulmonary retention, and enhanced systemic exposure. These properties may significantly improve patient compliance and therapeutic effectiveness in tuberculosis management. Nevertheless, further long-term toxicity studies, pulmonary deposition studies, and clinical investigations are necessary to

Table 4: Pharmacokinetic parameters of isoniazid, rifampicin, moxifloxacin HCl, and pyrazinamide following administration as conventional solutions and as nanoparticle-loaded in situ gel formulations (mean ± SD).

Parameter	Unit	Pharmacokinetic parameters							
		Isoniazid solution	Rifampicin solution	Moxifloxacin HCl Solution	Pyrazinamide Solution	Isoniazid nanoparticle in situ gel	Rifampicin nanoparticle in situ gel	Moxifloxacin HCl nanoparticle in situ gel	Pyrazinamide nanoparticle in situ gel
t1/2	h	1.441±0.020	5.326±0.437	14.676±0.586	9.018±0.206	21.341±0.798	22.591±1.110	29.088±2.606	29.339±0.977
T_{max}	h	2.000±0.00	4.000±0.00	6.000±0.00	6.000±0.00	12.000±0.000	12.000±0.00	12.000±0.000	12.000±0.00
C_{max}	µg/mL	1.912±0.071	19.10±2.1360	73.594±2.899	49.339±2.847	124.588±2.907	182.116±1.844	426.72±48.337	951.14±32.1137
AUC_{0-t}	µg/mL*h	10.718±0.262	204.014±26.319	1779.471±66.848	1271.445±68.44	3680.051±111.276	5409.974±73.924	11296.888±145.708	29019.999±1002.250
AUC_{0-inf_obs}	µg/mL*h	10.791±0.265	214.394±27.773	1981.079±71.677	1297.603±67.008	4853.502±136.341	7397.471±151.370	18588.078±1242.69	46108.117±2510.927
Vz/F_obs	(mg/kg)/(µg/mL)	1.485±0.031	0.560±0.093	0.440±0.019	0.413±0.032	0.049±0.002	0.068±0.002	0.093±0.002	0.038±0.001
Cl/F_obs	(mg/kg)/(µg/mL)/h	0.715±0.018	0.073±0.010	0.021±0.01	0.032±0.0002	0.002±0.000	0.002±0.00	0.002±0.00	0.001±0.000

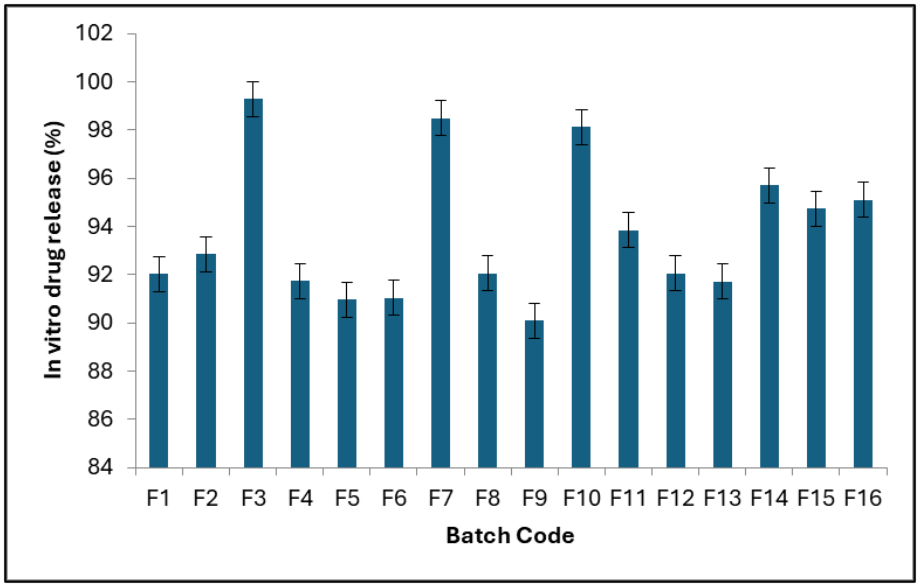

Figure 8: *In vitro* drug release profiles (%) of nanoparticle-loaded *in situ* gel formulations (G1-G4) evaluated using a Franz diffusion cell with dialysis membrane (MWCO 12,000-14,000 Da) in phosphate-buffered saline (pH 7.4) at 37 ± 0.5ºC and 100 rpm for 12 hr (mean ± SD, *n* = 3). Formulation G3 exhibited sustained and controlled drug release.

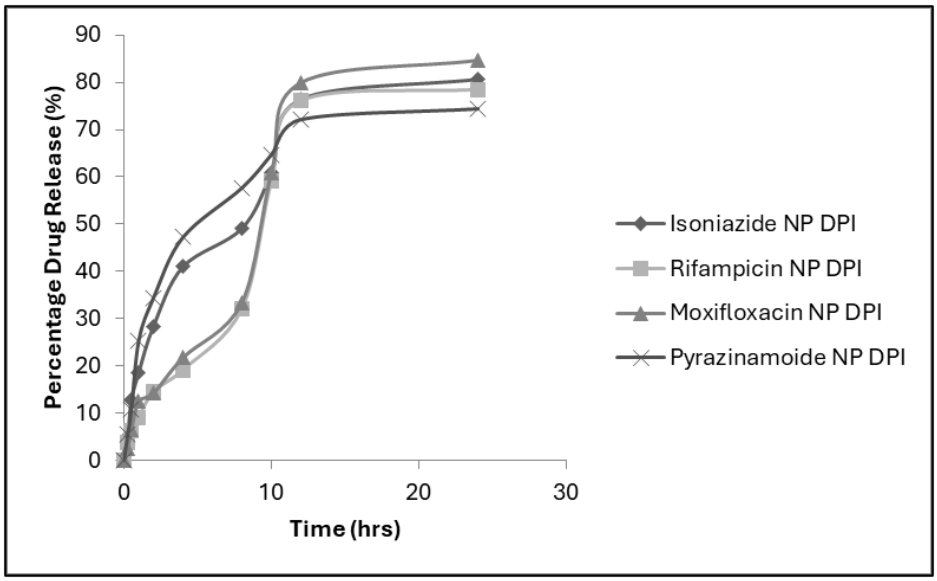

Figure 9: Comparative *in vitro* drug release profiles of optimized nanoparticle-loaded *in situ* gel formulation (G3) and corresponding nanoparticle-based dry powder inhaler (DPI) formulation under identical release conditions (PBS pH 7.4, 37 ± 0.5ºC). The thermosensitive gel demonstrated more controlled and sustained release behavior compared to DPI formulation.

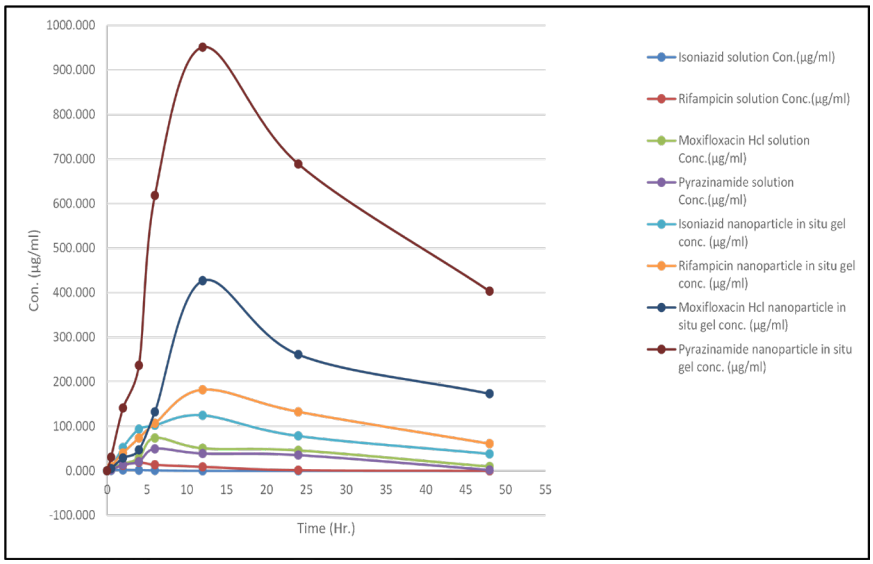

Figure 10: Extended *in vitro* drug release comparison over 48 hr between pure drug solutions and nanoparticle-loaded thermosensitive *in situ* gel formulations under simulated physiological conditions (PBS pH 7.4, 37 ± 0.5ºC). Nanoparticle-loaded gels exhibited reduced burst release and prolonged drug retention compared to conventional drug solutions.

establish the safety and clinical applicability of the developed system for future translational use.

CONCLUSION

The developed nanoparticle-loaded thermosensitive *in situ* gel system for anti-tubercular drugs demonstrated improved drug encapsulation, sustained pulmonary release, enhanced bioavailability, prolonged systemic exposure, and better pharmacokinetic performance compared to conventional formulations. DSC and XRD studies confirmed successful drug encapsulation with partial amorphization of the drugs. The formulation showed extended drug release, increased half-life and AUC, along with reduced clearance, indicating improved therapeutic efficacy and reduced dosing frequency. This advanced pulmonary delivery system holds strong potential for improving patient compliance and therapeutic outcomes in tuberculosis treatment, warranting further clinical evaluation.

ACKNOWLEDGEMENT

The authors acknowledge the support from DIT University, Dehradun.

ABBREVIATIONS

TB: Tuberculosis; **HPMC:** Hydroxypropyl Methylcellulose; **DPI:** Dry Powder Inhaler; **FTIR:** Fourier Transform Infrared Spectroscopy; **DSC:** Differential Scanning Calorimetry; **ATDs:** Anti-Tubercular Drugs; **XRD:** X-ray Diffraction; **PXRD:** Powder X-ray Diffraction; **HCl:** Hydrochloride; **PBS:** Phosphate-Buffered Saline; **MWCO:** Molecular Weight Cut-Off; **DEE:** Drug Entrapment Efficiency; **SD:** Standard Deviation; **IAEC:** Institutional Animal Ethics Committee; **CCSEA:** Committee for the Control and Supervision of Experiments on Animals; **HPLC:** High-Performance Liquid Chromatography; **INH:** Isoniazid; **PZA:** Pyrazinamide; **MRT:** Mean Residence Time; **C_{max}:** Maximum Plasma Concentration; **T_{max}:** Time to Reach Maximum Plasma Concentration; **AUC_{0-t}:** Area Under the Plasma Concentration–Time Curve from Zero to Last Measurable Time Point; **$AUC_{0-\infty}$:** Area Under the Plasma Concentration–Time Curve from Zero to Infinity; **rpm:** Revolutions Per Minute; **w/v:** Weight per Volume; **w/w:** Weight per Weight; **mM:** Millimolar; **µm:** Micrometre; **µL:** Microlitre; **°C:** Degrees Celsius; **cps:** Centipoise; **pH:** Potential of Hydrogen.

CONFLICT OF INTEREST

The authors declare that there is no conflict of interest.

AUTHOR CONTRIBUTIONS

Concept and Design: PS, BK, and SKV; Data Acquisition: PS; Data analysis/interpretation: PS and BK; Drafting manuscript: PS, BK; Writing - review and editing: BK and SKV; Supervision: BK and SKV.

REFERENCES

A, S., Ahmed, M. G., & Gowda BH, J. (2021). Preparation and evaluation of *in situ* gels containing hydrocortisone for the treatment of aphthous ulcer. *Journal of Oral Biology and Craniofacial Research*, *11*(2), 269-276. doi: 10.1016/J.JOBCR.2021.02.001

Ahmad, Z., Sharma, S., & Khuller, G. K. (2005). *In vitro* and *ex vivo* antimycobacterial potential of azole drugs against Mycobacterium tuberculosis H37Rv. *FEMS Microbiology Letters*, *251*(1), 19-22. doi: 10.1016/J.FEMSLE.2005.07.022

Ahmad, Z., Sharma, S., & Khuller, G. K. (2006). Azole antifungals as novel chemotherapeutic agents against murine tuberculosis. *FEMS Microbiology Letters*, *261*(2), 181-186. doi: 10.1111/J.1574-6968.2006.00350.X;PAGE:STRING:ARTICLE/CHAPTER

Al-Amin, K., Kawsar, M., Mamun, M. T. R. B., & Sahadat Hossain, M. (2025). Fourier transform infrared spectroscopic technique for analysis of inorganic materials: a review. *Nanoscale Advances*, *7*(21), 6677. doi: 10.1039/D5NA00522A

Ali, M. H., Azad, M. A. K., Khan, K. A., Rahman, M. O., Chakma, U., & Kumer, A. (2023). Analysis of Crystallographic Structures and Properties of Silver Nanoparticles Synthesized Using PKL Extract and Nanoscale Characterization Techniques. *ACS Omega*, *8*(31), 28133. doi: 10.1021/ACSOMEGA.3C01261

Balu, P., Srikanth, S., Gnandhas, D. P., Durai, R. D., Ulaganathan, V., & B Narayanan, V. H. (2025). Development and optimization of an injectable *in situ* gel system for sustained release of anti-tuberculosis drugs. *Scientific Reports 2025 15: 1*, *15*(1),21383-. doi: 10.1038/s41598-025-05644-3

Bekker, A., Schaaf, H. S., Draper, H. R., Van Ser Laan, L., Murray, S., Wiesner, L., Donald, P. R., Mcilleron, H. M., & Hesseling, A. C. (2016). Pharmacokinetics of Rifampin, Isoniazid, Pyrazinamide, and Ethambutol in Infants Dosed According to Revised WHO-Recommended Treatment Guidelines. *Antimicrobial Agents and Chemotherapy*, *60*(4), 2171. doi: 10.1128/AAC.02600-15

Cojocaru, E., Petriș, O. R., & Cojocaru, C. (2024). Nanoparticle-Based Drug Delivery Systems in Inhaled Therapy: Improving Respiratory Medicine. *Pharmaceuticals (Basel, Switzerland)*, *17*(8). doi: 10.3390/PH17081059

El-Houssiny, A. S., Ward, A. A., Mostafa, D. M., Abd-El-Messieh, S. L., Abdel-Nour, K. N., Darwish, M. M., & Khalil, W. A. (2016). Drug-polymer interaction between glucosamine sulfate and alginate nanoparticles: FTIR, DSC and dielectric spectroscopy studies. *Advances in Natural Sciences: Nanoscience and Nanotechnology*, *7*(2), 025014. doi: 10.1088/2043-6262/7/2/025014

Garala, K., Joshi, P., Patel, J., Ramkishan, A., & Shah, M. (2013). Formulation and evaluation of periodontal *in situ* gel. *International Journal of Pharmaceutical Investigation*, *3*(1), 29. doi: 10.4103/2230-973X.108961

Gebreel, R. M., Edris, N. A., Elmofty, H. M., Tadros, M. I., El-Nabarawi, M. A., & Hassan, D. H. (2021). Development and Characterization of PLGA Nanoparticle-Laden Hydrogels for Sustained Ocular Delivery of Norfloxacin in the Treatment of Pseudomonas Keratitis: An Experimental Study. *Drug Design, Development and Therapy*, *15*, 399. doi: 10.2147/DDDT.S293127

Gerber, T., Taschner-Mandl, S., Saloberger-Sindhöringer, L., Popitsch, N., Heitzer, E., Witt, V., Geyeregger, R., Hutter, C., Schwentner, R., Ambros, I. M., & Ambros, P. F. (2020). Assessment of Pre-Analytical Sample Handling Conditions for Comprehensive Liquid Biopsy Analysis. *The Journal of Molecular Diagnostics*, *22*(8), 1070-1086. doi: 10.1016/J.JMOLDX.2020.05.006

Gill, P., Moghadam, T. T., & Ranjbar, B. (2010). Differential Scanning Calorimetry Techniques: Applications in Biology and Nanoscience. *Journal of Biomolecular Techniques : JBT*, *21*(4), 167. Retrieved from https://pmc.ncbi.nlm.nih.gov/articles/PMC2977967/

Hirun, N., Kraisit, P., & Tantishaiyakul, V. (2022). Thermosensitive Polymer Blend Composed of Poloxamer 407, Poloxamer 188 and Polycarbophil for the Use as Mucoadhesive *In situ* Gel. *Polymers* 2022, *Vol. 14*, *14*(9). doi: 10.3390/POLYM14091836

Hui-Hui, Z., Qiu-Hua, L., Zhi-Jun, Y., Wei-San, P., & Shu-Fang, N. (2011). Novel ophthalmic timolol meleate liposomal-hydrogel and its improved local glaucomatous therapeutic effect *in vivo*. *Drug Delivery*, *18*(7), 502-510. doi: 10.3109/10717544.2011.595839;PAGE:STRING:ARTICLE/CHAPTER

Ingham, B. (2015). X-ray scattering characterisation of nanoparticles. *Crystallography Reviews*, *21*(4), 229-303. doi: 10.1080/0889311X.2015.1024114;REQUESTEDJOURNAL:JOURNAL:GCRY20;WGROUP:STRING:PUBLICATION

Jeswani, G., Chablani, L., Gupta, U., Sahoo, R. K., Nakhate, K. T., & Ajazuddin. (2021). Development and optimization of paclitaxel loaded Eudragit/PLGA nanoparticles by simplex lattice mixture design: Exploration of improved hemocompatibility and *in vivo* kinetics. *Biomedicine & Pharmacotherapy*, *144*, 112286. doi: 10.1016/J.BIOPHA.2021.112286

Karemore, M. N., & Avari, J. G. (2019). *In situ* gel of nifedipine for preeclampsia: Optimization, *in vitro* and *in vivo* evaluation. *Journal of Drug Delivery Science and Technology*, *50*, 78-89. doi: 10.1016/J.JDDST.2019.01.025

Kattar, A., Vivero-Lopez, M., Concheiro, A., Mudakavi, R., Chauhan, A., & Alvarez-Lorenzo, C. (2024). Oleogels for the ocular delivery of epalrestat: formulation, *in vitro*, in ovo, *ex vivo* and *in vivo* evaluation. *Drug Delivery and Translational Research*, *14*(11), 3291. doi: 10.1007/S13346-024-01560-7

Kim, J., & Jesus, O. De. (2023). Medication Routes of Administration. *StatPearls*. Retrieved from https://www.ncbi.nlm.nih.gov/books/NBK568677/

Kumar, D., Jain, N., Gulati, N., & Nagaich, U. (2013). Nanoparticles laden *in situ* gelling system for ocular drug targeting. *Journal of Advanced Pharmaceutical Technology & Research*, *4*(1), 9-17. doi: 10.4103/2231-4040.107495

Kumar, M., Virmani, T., Kumar, G., Deshmukh, R., Sharma, A., Duarte, S., Brandão, P., & Fonte, P. (2023). Nanocarriers in Tuberculosis Treatment: Challenges and Delivery Strategies. *Pharmaceuticals*, *16*(10), 1360. doi: 10.3390/PH16101360

Kumar Subramani, P., P N, R., & Narayanasamy, D. (2024). The Role of Pulmonary Drug Delivery in Modern Therapeutics: An Overview. *Cureus*, *16*(9). doi: 10.7759/CUREUS.68639

Nair, A., Greeny, A., Nandan, A., Sah, R. K., Jose, A., Dyawanapelly, S., Junnuthula, V., Athira, K. V., & Sadanandan, P. (2023). Advanced drug delivery and therapeutic strategies for tuberculosis treatment. *Journal of Nanobiotechnology*, *21*(1). doi: 10.1186/S12951-023-02156-Y

Nakmode, D. D., Singh, B., Abdella, S., Song, Y., & Garg, S. (2024). Long-acting parenteral formulations of hydrophilic drugs, proteins, and peptide therapeutics: mechanisms, challenges, and therapeutic benefits with a focus on technologies. *Drug Delivery and Translational Research 2024 15: 4*, *15*(4),1156-1180. doi: 10.1007/S13346-024-01747-Y

Nasra, M. M. A., Khiri, H. M., Hazzah, H. A., & Abdallah, O. Y. (2017). Formulation, *in vitro* characterization and clinical evaluation of curcumin *in situ* gel for treatment of periodontitis. *Drug Delivery*, *24*(1), 133. doi: 10.1080/10717544.2016.1233591

Pasieczna-Patkowska, S., Cichy, M., & Flieger, J. (2025). Application of Fourier Transform Infrared (FTIR) Spectroscopy in Characterization of Green Synthesized Nanoparticles. *Molecules* 2025, Vol. 30 *Page 684*, *30*(3), 684. doi: 10.3390/MOLECULES30030684

Patel, K., Patel, A., Jethwa, V. P., Patel, H., & Solanki, G. K. (2024). X-ray diffraction analysis of orthorhombic SnSe nanoparticles by Williamson-Hall, Halder-Wagner and Size-Strain plot methods. *Chemical Physics Impact*, *8*, 100547. doi: 10.1016/J.CHPHI.2024.100547

Petrashen, A. P., Verdesca, A. D., Kreiling, J. A., & Sedivy, J. M. (2023). Regulation of the somatotropic axis by MYC-mediated miRNA repression. *Frontiers in Cell and Developmental Biology*, *11*, 1269860. doi: 10.3389/FCELL.2023.1269860/BIBTEX

Presbítero-Espinosa, G., Peña-Parás, L., Sánchez-Fernández, J. A., Pizaña, E. I. R., Galván, K. P. V., Vopálenský, M., Kumpová, I., & Elizalde-Herrera, L. E. (2021). Characterization of Sodium Alginate Hydrogels Reinforced with Nanoparticles of Hydroxyapatite for

Biomedical Applications. *Polymers 2021,* Vol. 13 *Page 2927*, *13*(17), 2927. doi: 10.3390/POLYM13172927

Ramachandran, G., Kumar, A. K. H., Kannan, T., Thangakunam, B., Shankar, D., & Christopher, D. J. (2023). Pharmacokinetics of rifampicin, isoniazid & pyrazinamide during daily & intermittent dosing: A preliminary study. *The Indian Journal of Medical Research*, *157*(2-3), 211. doi: 10.4103/IJMR.IJMR_1835_19

Rosiak, N., Tykarska, E., & Cielecka-Piontek, J. (2023). The Study of Amorphous Kaempferol Dispersions Involving FT-IR Spectroscopy. *International Journal of Molecular Sciences*, *24*(24), 17155. doi: 10.3390/IJMS242417155/S1

Salem, H. F., Nafady, M. M., Eissa, E. M., Abdel-Sattar, H. H., & Khallaf, R. A. (2024). Assembly of *In situ* Gel Containing Nano-Spanlastics of an Angiotensin II Inhibitor as a Novel Epitome for Hypertension Management: Factorial Design Optimization, *In vitro* Gauging, Pharmacokinetics, and Pharmacodynamics Appraisal. *AAPS PharmSciTech 2024 25: 5*, *25*(5),115-. doi: 10.1208/S12249-024-02823-9

Sebe, I., Zsidai, L., & Zelkó, R. (2022). Novel modified vertical diffusion cell for testing of *in vitro* drug release (IVRT) of topical patches. *HardwareX*, *11*. doi: 10.1016/j.ohx.2022.e00293

Sun, Z., Peng, X., Yang, L., Liu, W., Liu, W., Du, X., Zhuo, J., Bao, B., Zhou, C., & Xiong, H. (2025). Folate-modified nanodelivery platform loaded with triptolide for targeted synergistic photothermal therapy of macrophages to alleviate rheumatoid arthritis. *Materials & Design*, *258*, 114619. doi: 10.1016/J.MATDES.2025.114619

Tripathi, M., Gharti, L., Bansal, A., Kaurav, H., & Sheth, S. (2025). Intranasal Mucoadhesive *In situ* Gel of Glibenclamide-Loaded Bilosomes for Enhanced Therapeutic Drug Delivery to the Brain. *Pharmaceutics*, *17*(2), 193. doi: 10.3390/PHARMACEUTICS17020193/S1

Ullah, K. H., Raza, F., Munawar, M., Sohail, M., Zafar, H., Zafar, M. I., & Ur-rehman, T. (2021). Poloxamer 407 based gel formulations for transungual delivery of hydrophobic drugs: Selection and optimization of potential additives. *Polymers*, *13*(19), 3376. doi: 10.3390/POLYM13193376/S1

Vigani, B., Rossi, S., Sandri, G., Bonferoni, M. C., Caramella, C. M., & Ferrari, F. (2020). Recent Advances in the Development of *In situ* Gelling Drug Delivery Systems for Non-Parenteral Administration Routes. *Pharmaceutics*, *12*(9), 1-29. doi: 10.3390/PHARMACEUTICS12090859

Wu, Y., Liu, Y., Li, X., Kebebe, D., Zhang, B., Ren, J., Lu, J., Li, J., Du, S., & Liu, Z. (2019). Research progress of *in situ* gelling ophthalmic drug delivery system. *Asian Journal of Pharmaceutical Sciences*, *14*(1), 1-15. doi: 10.1016/J.AJPS.2018.04.008

Zakaria, Z. A., Kamisan, F. H., Omar, M. H., Mahmood, N. D., Othman, F., Abdul Hamid, S. S., & Abdullah, M. N. H. (2017). Methanol extract of Dicranopteris linearis L. leaves impedes acetaminophen-induced liver intoxication partly by enhancing the endogenous antioxidant system. *BMC Complementary and Alternative Medicine* 2017 17:*1*, *17*(1), 271-. doi: 10.1186/S12906-017-1781-5

Zhang, Z., Zhang, Y., Wang, Q., & Ahmad, I. (2024). Characterization and performance evaluation of pH-sensitive drug delivery of nanoparticles prepared using green method with coating and capsule structure. *Journal of Molecular Liquids*, *397*, 124145. doi: 10.1016/J.MOLLIQ.2024.124145

Cite this article: Singh P, Kumar B, Verma SK. Poloxamer-Based Thermosensitive Nanoparticle *in situ* Gel for Sustained Pulmonary Anti-Tubercular Drug Delivery. J Young Pharm. 2026;18(3):741-54.